

A New Binding Motif of Sterically Demanding Thiolates on a Gold Cluster

Jun-ichi Nishigaki,[†] Risako Tsunoyama,[‡] Hironori Tsunoyama,[‡] Nobuyuki Ichikuni,[§] Seiji Yamazoe,[†] Yuichi Negishi,^{||} Mikinao Ito,[⊥] Tsukasa Matsuo,[⊥] Kohei Tamao,[⊥] and Tatsuya Tsukuda^{*,†,‡}

[†]Department of Chemistry, School of Science, The University of Tokyo, 7-3-1 Hongo, Bunkyo-ku, Tokyo 113-0033, Japan

[‡]Catalysis Research Center, Hokkaido University, Nishi 10, Kita 21, Sapporo 001-0021, Japan

[§]Department of Applied Chemistry and Biotechnology, Graduate School of Engineering, Chiba University, Inage-ku, Chiba 263-8522, Japan

^{||}Department of Applied Chemistry, Faculty of Science, Tokyo University of Science, 1-3 Kagurazaka, Shinjuku-ku, Tokyo 162-8601, Japan

[⊥]Functional Elemento-Organic Chemistry Unit, RIKEN Advanced Science Institute, 2-1 Hirosawa, Wako, Saitama 351-0198, Japan

Supporting Information

ABSTRACT: A gold cluster, Au₄₁(S-Eind)₁₂, was synthesized by ligating the bulky arenethiol 1,1,3,3,5,5,7,7-octaethyl-*s*-hydrindacene-4-thiol (Eind-SH) to preformed Au clusters. Extended X-ray absorption fine structure, X-ray photoelectron spectroscopy, and the fragmentation pattern in the mass spectrometry analysis indicated that formation of gold–thiolate oligomers at the interface was suppressed, in sharp contrast to conventional thiolate-protected Au clusters.

Crystallographic structure determination of Au₁₀₂(*p*-MBA)₄₄ (MBA = mercaptobenzoic acid) by Kornberg's group¹ has made a breakthrough in our understanding of the structure of thiolate-protected Au clusters (Au:SR). It was found that gold–thiolate oligomers, –SR–[Au–SR–] (named “staples”) and –SR–[Au–SR–]₂, are completely coordinated to a decahedral Au₇₉ core.² Subsequently, similar interfacial structures have been theoretically predicted and experimentally observed in Au₂₅(SR)₁₈ (ref 3) as well as Au₃₈(SR)₂₄.⁴ The formation of such oligomers has also been theoretically proposed for other isolated clusters, including Au₁₈(SR)₁₄,⁵ Au₂₀(SR)₁₆,^{5–7} Au₂₄(SR)₂₀,⁸ Au₄₄(SR)₂₈,⁹ and Au₁₄₄(SR)₆₀.¹⁰ Gold–thiolate oligomeric interfacial structures have a big impact on the physicochemical properties of small Au:SR, such as magnetism,¹¹ photoluminescence,¹² chiroptical activity,¹³ and catalysis.¹⁴

New properties can emerge from the construction of new interfacial structures in Au:SR. In a previous study, we intended to ligate the thiolates directly on the surface of the Au core by reacting *n*-alkanethiol with preformed Au clusters weakly stabilized by poly(*N*-vinyl-2-pyrrolidone) (PVP).¹⁵ However, the structure of the Au core was substantially reconstructed in the ligation process, and Au–SR oligomers were formed at the interface. In this study, the bulky, rigid arenethiols 1,1,3,3,5,5,7,7-octaethyl-*s*-hydrindacene-4-thiol (Eind-SH) and 3,3,5,5-tetraethyl-1,1,7,7-tetramethyl-*s*-hydrindacene-4-thiol (MEind-SH) (Figure 1) were employed as protecting ligands.^{16,17} Two modes of the steric effect are expected for

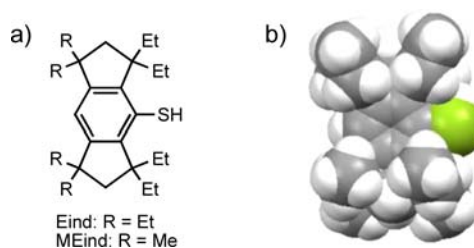


Figure 1. (a) Molecular structures of Eind-SH and MEind-SH. (b) Space-filling model of Eind-SH. The green ball represents the sulfur atom.

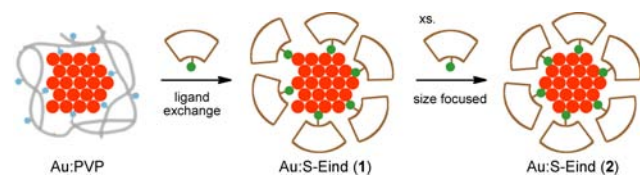
these bulky arenethiols. One is the steric repulsion between adjacent ligands. This should reduce the coverage of the ligand and/or the size of the Au clusters; Tracy and co-workers demonstrated that Au clusters protected by bulky thiolate (1-adamantanethiolate and cyclohexanethiolate) have slightly smaller coverage of the ligands and that bulkier ligands afforded smaller sizes of Au–thiolate clusters.¹⁸ The other effect is the steric constraint around the sulfur group. This should suppress the formation of Au–SR oligomers on the Au cluster surface. Here we report the formation of a new binding motif of the bulky Eind thiolate on a Au₄₁ cluster.

Details of the synthesis of Au clusters protected by the Eind- and MEind-thiolates (Au:S-Eind and Au:S-MEind) are described in the Supporting Information (SI);¹⁷ only the general synthetic method for Au:S-Eind is described below. We initially attempted to prepare Au:S-Eind by the Brust method.¹⁹ However, this method yielded precipitates and nanoparticles larger than ~2 nm as major products. Next, the ligand exchange approach was employed; Au_n clusters stabilized by PVP (Au_n:PVP) were allowed to react with Eind-SH in toluene (Scheme 1).¹⁷ An aqueous dispersion of Au_n:PVP (*n* ≈ 38; Figure S1 in the SI) was mixed with a toluene solution of Eind-SH by either batch or microfluidic mixing at 90 °C. The intense dark-brown color of the water phase was transferred to the

Received: June 6, 2012

Published: August 17, 2012

Scheme 1. Synthesis of Au:S-Eind (1 and 2)



toluene phase, indicating the efficient formation of Au:S-Eind. The yield of Au:S-Eind obtained using the micromixer was higher by $\sim 10\%$ than that prepared by batch mixing (Figure S2). This indicates that ligation proceeded more efficiently by microfluidic mixing than by batch mixing, probably because of more homogeneous and rapid mixing of the two phases. The size distribution of the crude Au:S-Eind extracted in toluene (1) was focused²⁰ by incubating it in the presence of excess Eind-SH in toluene. Au:S-Eind (2) was isolated by removal of excess Eind-SH by size-exclusion chromatography (Figure S3) and dried under vacuum. Clusters 2 did not decompose for at least several days when stored at $-20\text{ }^\circ\text{C}$ in a powder form.

Clusters 2 were characterized in detail by various methods. Transmission electron microscopy (TEM) observation (Figure S4) indicated that an average diameter of the Au core was $1.3 \pm 0.3\text{ nm}$. Powder X-ray diffraction confirmed the formation of small Au(0) clusters (Figure S5). Figure 2 shows a matrix-

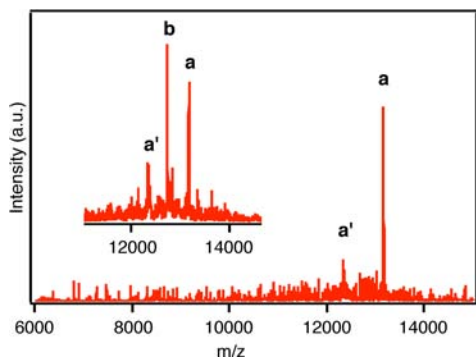


Figure 2. Typical MALDI-TOF mass spectrum of Au:S-Eind (2). The inset shows the mass spectrum of the crude sample of Au:S-Eind (1).

assisted laser desorption ionization-time-of-flight (MALDI-TOF) mass spectrum of 2 in the negative-ion mode recorded at low laser power to minimize fragmentation. The mass spectrum contains two sharp peaks, a and a', at m/z 13117 and 12295, respectively. On the basis of the power dependence (Figure S6), we assigned peak a to the main species present in sample 2 and peak a' to a fragment of a produced during the MALDI process. An additional peak, b, at m/z 12680 observed in the crude sample 1 (Figure 2 inset) disappeared upon etching with excess Eind-SH.

The parent peak a was assigned to $\text{Au}_{41}(\text{S-Eind})_{12}$ by comparing the mass spectra of Au:S-Eind and Au:S-MEind (Figure S7); the number of ligands was determined from the mass difference between the corresponding peaks, and the number of Au atoms was then determined from the molecular weight of the cluster. The formation of the Au_{41} core was confirmed by the detection of an intense fragment peak of Au_{41}^- in the MALDI-TOF mass spectrum recorded at high laser power (Figure S8) and is consistent with the average size determined by TEM (Figure S4). Thermogravimetric analysis

(Figure S9) indicated that the Au ratio was $63.2 \pm 1.0\%$, which is consistent with that calculated for $\text{Au}_{41}(\text{S-Eind})_{12}$ (61.9%). Peak a' was assigned to $\text{Au}_{41}(\text{S-Eind})_{10}$, which is produced by release of two Eind-S ligands (probably in the form of a disulfide) from $\text{Au}_{41}(\text{S-Eind})_{12}$. Peak b was assigned to $\text{Au}_{43}(\text{S-Eind})_{10}$. The poorer stability of $\text{Au}_{43}(\text{S-Eind})_{10}$ compared with $\text{Au}_{41}(\text{S-Eind})_{12}$ against etching is associated with lower coverage. The formation of $\text{Au}_{41}(\text{S-Eind})_{12}$ and $\text{Au}_{43}(\text{S-Eind})_{10}$ in the crude sample 1 was confirmed by the observation of Au_{41}^- and Au_{43}^- in the MALDI-TOF mass spectra (Figure S8). However, we note that the observed masses for a and a' were larger than those calculated for $\text{Au}_{41}(\text{S-Eind})_{12}$ and $\text{Au}_{41}(\text{S-Eind})_{10}$ by $\sim 80\text{ Da}$ (Table S1 in the SI). This result implies that the clusters contain additional species such as oxygen or sulfur.

The gold-thiolate interfacial structure of $\text{Au}_{41}(\text{S-Eind})_{12}$ is significantly different from that of conventional Au:SR, as discussed below. First, the thiolate coverage of $\text{Au}_{41}(\text{S-Eind})_{12}$ is remarkably smaller than those of other Au:SR reported to date. Figure 3 compares the thiolate-to-Au ratio in $\text{Au}_{41}(\text{S-}$

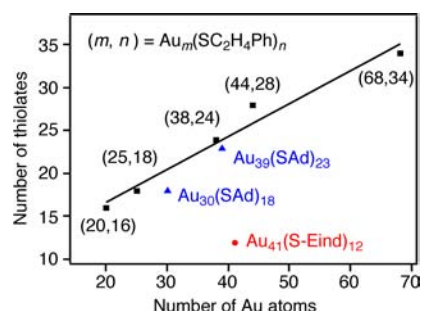


Figure 3. Compositions of $\text{Au}_{41}(\text{S-Eind})_{12}$, $\text{Au}_m(\text{SAD})_n$, and $\text{Au}_m(\text{SC}_2\text{H}_4\text{Ph})_n$.^{18,21}

$\text{Eind})_{12}$ with those in Au clusters protected by *n*-alkanethiolates, phenylethanethiolates, and 1-adamantanethiolate (SAd).^{18,21} The much smaller thiolate-to-Au ratio for $\text{Au}_{41}(\text{S-Eind})_{12}$ is due to steric repulsion between the ligands. Second, Eind-S and Au do not form oligomers at the interface of $\text{Au}_{41}(\text{S-Eind})_{12}$, in sharp contrast to conventional Au:SR. Extended X-ray absorption fine structure (EXAFS) analysis (Figure 4a) revealed that the Au-Au coordination number (CN) of $\text{Au}_{41}(\text{S-Eind})_{12}$ was 4.1 ± 0.4 , which is much larger than that of $\text{Au}_{38}(\text{SC}_{18}\text{H}_{37})_{24}$ (1.7 ± 0.2) but comparable to that of $\text{Au}_{\sim 43}:\text{PVP}$ (4.4 ± 0.4).²² This result indicates that all of the constituent Au atoms of $\text{Au}_{41}(\text{S-Eind})_{12}$ create a core, as in the case of $\text{Au}_{\sim 43}$ stabilized by PVP. The average CN for the Au-S shell of $\text{Au}_{41}(\text{S-Eind})_{12}$ was 0.9 ± 0.4 , indicating that an S-Eind is bound to three Au atoms on average ($0.9 \times 41/12 = 3.0$) through μ^3 -like bonding.²³ Third, the Au($4f_{7/2}$) electron binding energy of $\text{Au}_{41}(\text{S-Eind})_{12}$ was determined by X-ray photoelectron spectroscopy (XPS) to be 83.9 eV (Figure 4b), which is significantly smaller than those of conventional Au:SR²¹ and comparable to that of bulk Au (84.0 eV). Fourth, the fragmentation pattern of $\text{Au}_{41}(\text{S-Eind})_{12}$ was different from those of conventional Au:SR (Figure 4c). The loss of $(\text{S-Eind})_2$ was observed for $\text{Au}_{41}(\text{S-Eind})_{12}$, whereas the loss of $[\text{Au}_4(\text{SC}_{18}\text{H}_{37})_4 + \text{C}_{18}\text{H}_{37}]$ is the major fragmentation channel for $\text{Au}_{38}(\text{SC}_{18}\text{H}_{37})_{24}$.²⁴ The above discussion suggests that the 12 Eind-S ligands are directly bound to the Au_{41} core. Recently, Jiang and Walter theoretically predicted two types of stable structures for Au_{40} having twisted pyramid motifs: one has C_1

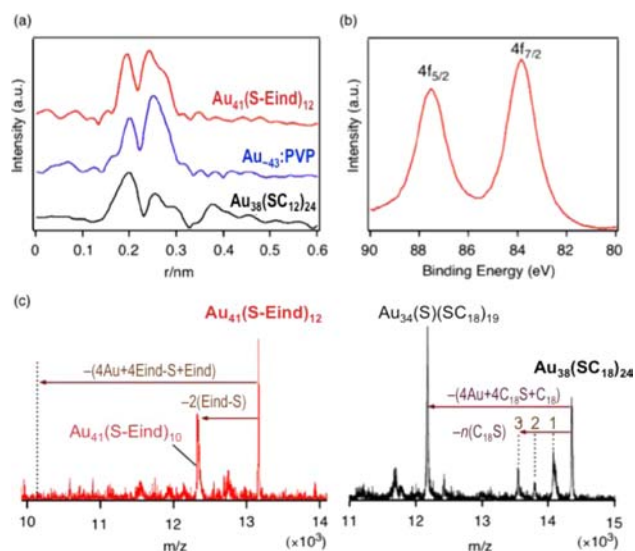


Figure 4. (a) Fourier transforms of the Au L_3 -edge EXAFS spectra, (b) XPS spectra, and (c) MALDI-TOF mass spectra of $\text{Au}_{41}(\text{S-Eind})_{12}$ (red), $\text{Au}_{43}\text{:PVP}$ (blue), and $\text{Au}_{38}(\text{SC}_{12})_{24}$ (black). C_{12} and C_{18} represent the $\text{C}_{12}\text{H}_{25}$ and $\text{C}_{18}\text{H}_{37}$ groups, respectively.

symmetry with a missing atom at the corner, and the other has C_3 symmetry with a missing atom at the core.²⁵ On the basis of these results, we proposed that the Au_{41} core has a twisted pyramid structure with a Au_4 core (Figure S10). To test this hypothesis, we studied the structural motif of the Au core by TEM. We frequently observed angular particles (triangles and squares), whereas only spherical particles were observed for $\text{Au}_{38}(\text{SC}_{12}\text{H}_{25})_{24}$ (Figure S11). This observation supports the formation of the twisted pyramid structure shown in Figure S10, although the structures could not be determined unambiguously because of electron-beam-induced structural fluctuations during the measurement.

In summary, we obtained size-selected gold clusters protected by the bulky Eind-thiolate ligand having the formula $\text{Au}_{41}(\text{S-Eind})_{12}$. The thiolate coverage is remarkably smaller than those in conventional Au:SR because of steric effects. EXAFS analysis, XPS, and the fragmentation pattern in the mass spectrometry analysis suggested that the formation of Au-thiolate oligomers is suppressed in $\text{Au}_{41}(\text{S-Eind})_{12}$, in sharp contrast to the hitherto-known Au:SR. Further studies of the structure and physicochemical properties are in progress.

■ ASSOCIATED CONTENT

Supporting Information

Details of synthesis and characterization. This material is available free of charge via the Internet at <http://pubs.acs.org>.

■ AUTHOR INFORMATION

Corresponding Author

tsukuda@chem.s.u-tokyo.ac.jp

Notes

The authors declare no competing financial interest.

■ ACKNOWLEDGMENTS

This research was financially supported by the Funding Program for Next Generation World-Leading Researchers (NEXT Program) (GR-003).

■ REFERENCES

- Jadzinsky, P. D.; Calero, G.; Ackerson, C. J.; Bushnell, D. A.; Kornberg, R. D. *Science* **2007**, *318*, 430.
- Walter, M.; Akola, J.; Lopez-Acevedo, O.; Jadzinsky, P. D.; Calero, G.; Ackerson, C. J.; Whetten, R. L.; Grönbeck, H.; Häkkinen, H. *Proc. Natl. Acad. Sci. U.S.A.* **2008**, *105*, 9157.
- (a) Heaven, M. W.; Dass, A.; White, P. S.; Holt, K. M.; Murray, R. W. *J. Am. Chem. Soc.* **2008**, *130*, 3754. (b) Zhu, M.; Aikens, C. M.; Hollander, F. J.; Schatz, G. C.; Jin, R. *J. Am. Chem. Soc.* **2008**, *130*, 5883. (c) Akola, J.; Walter, M.; Whetten, R. L.; Häkkinen, H.; Grönbeck, H. *J. Am. Chem. Soc.* **2008**, *130*, 3576.
- (a) Lopez-Acevedo, O.; Tsunoyama, H.; Tsukuda, T.; Häkkinen, H.; Aikens, C. M. *J. Am. Chem. Soc.* **2010**, *132*, 8210. (b) Qian, H.; Eckenhoff, W. T.; Zhu, Y.; Pintauer, T.; Jin, R. *J. Am. Chem. Soc.* **2010**, *132*, 8280. (c) Tlahuice, A.; Garzon, I. L. *Phys. Chem. Chem. Phys.* **2012**, *14*, 7321.
- Jiang, D.; Chen, W.; Whetten, R. L.; Chen, Z. *J. Phys. Chem. C* **2009**, *113*, 16983.
- Pei, Y.; Gao, Y.; Shao, N.; Zeng, X. C. *J. Am. Chem. Soc.* **2009**, *131*, 13619.
- Pei, Y.; Pal, R.; Liu, C.; Gao, Y.; Zhang, Z.; Zeng, X. C. *J. Am. Chem. Soc.* **2012**, *134*, 3015.
- Jiang, D.; Walter, M.; Akola, J. *J. Phys. Chem. C* **2010**, *114*, 15883.
- Lopez-Acevedo, O.; Akola, J.; Whetten, R. L.; Grönbeck, H.; Häkkinen, H. *J. Phys. Chem. C* **2009**, *113*, 5035.
- (a) Crespo, P.; Litrán, R.; Rojas, T. C.; Multigner, M.; de la Fuente, J. M.; Sánchez-López, J. C.; García, M. A.; Hernando, A.; Penadés, S.; Fernández, A. *Phys. Rev. Lett.* **2004**, *93*, No. 087204. (b) Yamamoto, Y.; Miura, T.; Suzuki, M.; Kawamura, N.; Miyagawa, H.; Nakamura, T.; Kobayashi, K.; Teranishi, T.; Hori, H. *Phys. Rev. Lett.* **2004**, *93*, No. 116801. (c) Negishi, Y.; Tsunoyama, H.; Suzuki, M.; Kawamura, N.; Matsushita, M.; Maruyama, K.; Sugawara, T.; Yokoyama, T.; Tsukuda, T. *J. Am. Chem. Soc.* **2006**, *128*, 12034.
- (a) Wang, G.; Huang, T.; Murray, R. W.; Menard, L.; Nuzzo, R. G. *J. Am. Chem. Soc.* **2005**, *127*, 812. (b) Devadas, M. S.; Kim, J.; Sinn, E.; Lee, D.; Goodson, T., III; Ramakrishna, G. *J. Phys. Chem. C* **2010**, *114*, 22417.
- (a) Yao, H.; Miki, K.; Nishida, N.; Sasaki, A.; Kimura, K. *J. Am. Chem. Soc.* **2005**, *127*, 15536. (b) Si, S.; Gautier, C.; Boudon, J.; Taras, R.; Gladiali, S.; Bürgi, T. *J. Phys. Chem. C* **2009**, *113*, 12966. (c) Shukla, N.; Bartel, M. A.; Gellman, A. J. *J. Am. Chem. Soc.* **2010**, *132*, 8575.
- Zhu, Y.; Qian, H.; Drake, B. A.; Jin, R. *Angew. Chem., Int. Ed.* **2010**, *49*, 1295.
- Tsunoyama, H.; Tsunoyama, H.; Pannopard, P.; Limtrakul, J.; Tsukuda, T. *J. Phys. Chem. C* **2010**, *114*, 16004.
- Matsuo, T.; Suzuki, K.; Fukawa, T.; Li, B.; Ito, M.; Shoji, Y.; Otani, T.; Li, L.; Kobayashi, M.; Hachiya, M.; Tahara, Y.; Hashizume, D.; Fukunaga, T.; Fukazawa, A.; Li, Y.; Tsuji, H.; Tamao, K. *Bull. Chem. Soc. Jpn.* **2011**, *84*, 1178.
- See the Supporting Information.
- Krommenhoek, P. J.; Wang, J.; Hentz, N.; Johnston-Peck, A. C.; Kozek, K. A.; Kalyuzhny, G.; Tracy, J. B. *ACS Nano* **2012**, *6*, 4903.
- Brust, M.; Walker, M.; Bethell, D.; Schiffrin, D. J.; Whyman, R. J. *Chem. Soc., Chem. Commun.* **1994**, 801.
- (a) Shichibu, Y.; Negishi, Y.; Tsunoyama, H.; Kanehara, M.; Teranishi, T.; Tsukuda, T. *Small* **2007**, *3*, 835. (b) Jin, R.; Qian, H.; Wu, Z.; Zhu, Y.; Zhu, M.; Mohanty, A.; Garg, N. *J. Phys. Chem. Lett.* **2010**, *1*, 2903.
- Maity, P.; Xie, S.; Yamauchi, M.; Tsukuda, T. *Nanoscale* **2012**, *4*, 4027 and references cited therein.
- Tsunoyama, H.; Tsukuda, T. *J. Am. Chem. Soc.* **2009**, *131*, 18216.
- (a) Luedtke, W. D.; Landman, U. *J. Phys. Chem.* **1996**, *100*, 13323. (b) Larsson, J. A.; Nolan, M.; Greer, J. C. *J. Phys. Chem. B* **2002**, *106*, 5931. (c) Nobusada, K. *J. Phys. Chem. B* **2004**, *108*, 11904.
- Qian, H.; Zhu, Y.; Jin, R. *ACS Nano* **2009**, *3*, 3795.
- Jiang, D.; Walter, M. *Phys. Rev. B* **2011**, *84*, No. 193402.